CHAPTER-V

EXPERIMENTAL RESULTS

In this chapter the results are given of the present experiments, done using NBU air shower array of 21 scintillation detectors with two shielded muon magnetic spectrographs, covering an area of about 1200 m^2 at sea level (1020 gm/cm^2).

The method of analysis of showers to obtain parameters (N_e, s, X_o, Y_o) and the momenta of muons is described in the chapter IV. The total shower data and muon data have been used to obtain the lateral distribution of muons in showers and finally the information on primary radiation. A sum of 17,067 showers with 1,229 muons are considered for the analysis given here. These results with possible errors in measurements of different parameters are given below.

5.1 Selection criteria

All showers with sizes less than the threshold size of 10^4 particles are rejected. Showers with reduced chi-square greater than 5 are rejected since these have doubtful parameters. Also the showers with age parameter less than 0.8 and greater than 1.3 are rejected since most of these showers are of small size with shower cores at large distances from the array. All the data have been primarily classified according to the estimated shower size.

5.2 Distribution of age parameter

Showers are grouped in bins of width of factor 2 in size. So that 7 bins of showers are considered in the size region $1 \times 10^4 \leqslant N_e \leqslant 1.2 \times 10^6$.

The mean value of age parameter(s) and the width of the age parameter (σ_s) for different shower sizes are presented in figure 5.1. The mean value ($\bar{s}$) is 1.27 at the size 10^4 particles and decreases to 0.91 at size 10^6 particles. The width of the distribution of age parameter (σ_s) also decreases from 0.18 to 0.1 over the same size range. The results of Akeno group[1] is shown by hatched area. They also used plastic scintillation detectors but only the detection area was different. The nature of variation of $\bar{s}$ with shower size is approximately similar for the size range 6×10^4 to 10^6 particles. Data points (closed circles) are from the KGF experiments[2]. There is a knee at the size range 4×10^4. In the present experiment there is no such knee but the value of $\bar{s}$ is very close to that at the lower shower size range.

5.3 Energy spectrum of primary cosmic rays

(a) Determination of shower size

21 scintillation detectors are used to determine the densities of electron at different points for a particular shower. In the present experiment only one type of triggering condition is

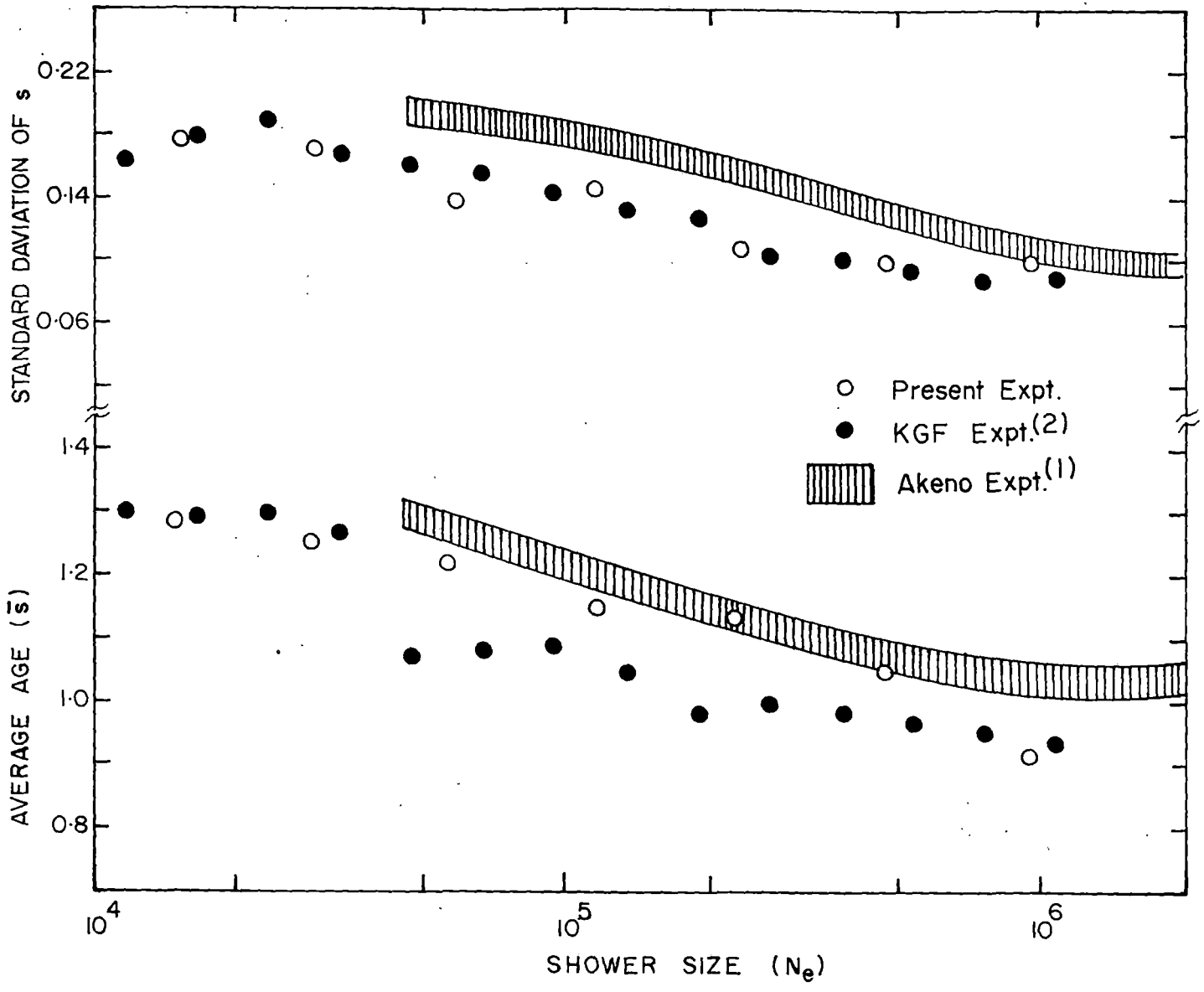

Fig. 5.1 VARIATION OF $\bar{s}$ AND σ_s WITH SHOWER SIZE

used for the collection of shower data. The triggering pulse is generated from the three-fold coincidence of the central 7 detectors [detector 1 to detector 7 (figure 3.1)]. The minimum required density for triggering is $4/m^2$ for 0.25 m^2 detectors and $8/m^2$ for 0.125 m^2 detectors. Number of particles at different detectors are recorded on a paper tape by a line printer. In the determination of observed densities the calibrated single particle pulse height for each detector is used to connect the recorded density into the number of particle per square metre. From the observed densities the shower size (N_e), shower age (s) and core position (r) are determined by χ^2 -minimisation procedure using Hillas[3] structure function.

(b) Estimation of flux

To obtain the primary spectrum all the showers in the size range 10^4 - 10^6 particles are divided into 7 size bins of width of factor 2 in size. Each shower size bin is also subdivided into 5 age bins of width 0.1. The radius R_{90} for 90% efficient area is obtained for the lower size limit for each bin. The frequency distribution of showers whose cores are within the radius R_{90} for s = 0.9 - 1.0 and 1.1 - 1.2 are shown in figure 5.2. The omni-directional flux can be written as

$$\frac{dF(N_i,s_j)}{dN_i ds_j} dN_i ds_j = \frac{n(N_i,s_j)}{TA(N_i,s_j)} \quad \ldots \quad (5.1)$$

where $n(N_i,s_j)$ is the number of showers collected for a period of time T in the ith size bin and j th age bin within R_{90}.

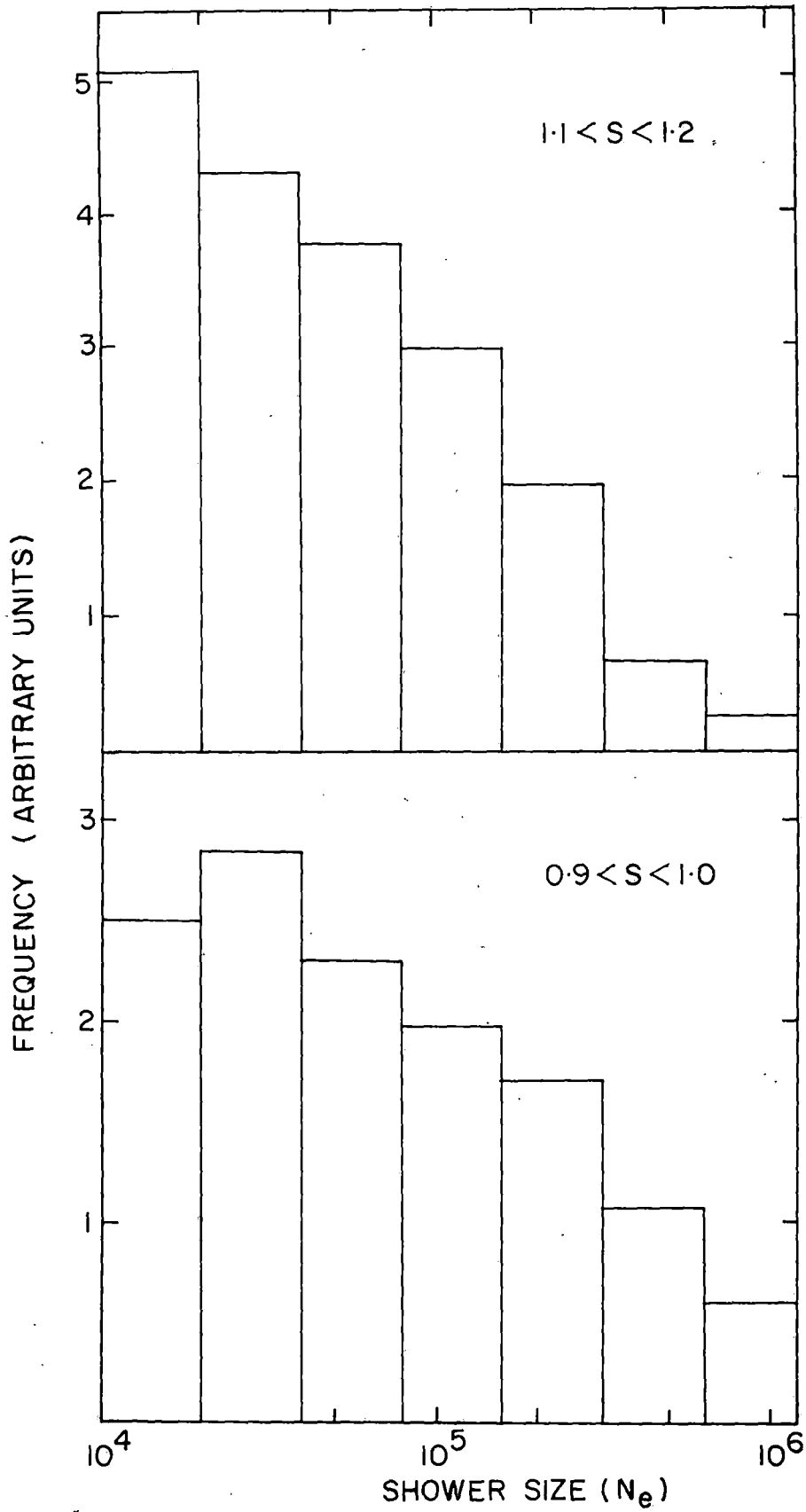

Fig. 5·2 FREQUENCY DISTRIBUTION OF SHOWERS WHOSE CORES ARE WITHIN R_{90}

From the study of showers of size $\sim 10^5$, it has been observed by Kameda et al[4] at 2770 m above the sea level and by McCusker[5] at sea level that the flux $F_\theta(N)$ coming at a zenith angle θ can be given in terms of the vertical flux $F_o(N)$ by the equation

$$F_\theta(N) = F_o(N)\mathrm{Cos}^n\theta \quad \ldots \quad \ldots \quad (5.2)$$

Kameda[4] and McCusker[5] found that the value of n is 6.7 ± 0.9 and ~ 8.3 respectively. Acharya[2] found n = 7 approximately at sea level in the size range $10^4 - 10^7$ particles. Thus the omni-directional flux is obtained from the vertical flux by integrating over all zenith angles and azimuthal angles as

$$F(N) = \int_0^{2\pi}\int_0^{\pi/2} F_o(N)\mathrm{Cos}^{n+1}\theta \sin\theta \, d\theta \, d\phi = \frac{2\pi}{n+2} F_o(N) \quad \ldots \quad (5.3)$$

Therefore the flux in the vertical direction is obtained as

$$\frac{dF_o(N_i,s_j)}{dN_i ds_j} dN_i ds_j = \frac{9}{2\pi T} \frac{n(N_i,s_j)}{A(N_i,s_j)} (m^2 \text{sec sr})^{-1} \quad \ldots \quad (5.4)$$

and thus the integral flux in the vertical direction can be obtained as

$$F_o(>N_i) = \frac{9}{2\pi T} \sum_i \sum_j \frac{n(N_i,s_j)}{A(N_i,s_j)} (m^2 \text{ sec sr})^{-1} \quad \ldots \quad (5.5)$$

(c) Estimation of primary energy from shower size

The electron size at the maximum shower development N (max) is well known as one of the best primary energy estimator which does not depend sensitively on interaction model nor primary composition. The conversion of the N(max) spectrum to the energy spectrum of primary cosmic rays is straight forward, since the primary energy (E_o) is related to the N (max) by a well defined relation

$$E_o = 1.6 \times 10^9 \times N(max) \text{ eV} \quad \ldots \quad (5.6)$$

The value of N (max) is estimated from the observed shower size by using the longitudinal development curve by Dedenko[6] and Akeno air shower experiment[7]. Using the distribution of primary energy for each size group, the primary energy is related to the shower size at depth 930 gm/cm^2 (Akeno experiment) by the equation

$$E_o = 3.9 \times 10^{15} \times \left(\frac{N_e}{10^6} \right)^{0.90} \text{ eV} \quad \ldots \quad (5.7)$$

In the present experiment we use the relation of TIFR group[8] based on Monte Carlo simulation. The equation is as follows.

$$E_o = (6.63 \pm 1.31) \times 10^{13} \left(\frac{N_e}{10^4} \right)^{0.81} \text{ eV} \quad \ldots \quad \ldots \quad (5.8)$$

for the shower size range 10^4 - 10^6 particles.

The integral energy spectrum from electron size is plotted in figure 5.3. The observed values are fitted with the equation of the form $F(\geq E_o) = K \left(\frac{E_o}{6.63 \times 10^{13}} \right)^{7-\alpha}$ $(m^2 \text{ sec sr})^{-1}$

where $K = (1.03 \pm 0.079) \times 10^{-4}$ and $\alpha = 1.611 \pm 0.057$

The error bars given on each point represent purely statistical errors and depend only on the number of observed showers.

5.4 Lateral distribution of electrons

All the showers in the size range 10^4-10^6 particles are recorded by 21 density sampling points. The observed densities at each detectors for a particular shower is determined by calibrating the detectors for single particle pulse height. Shower parameters N_e, s, X_o, Y_o are obtained from the observed densities by χ^2 -minimisation procedure using Hillas[3] structure function. The observed density is corrected by considering the effect of transition in the scintillator and its covering with the relation[9] $\Delta_c = \Delta_o$ (1.192 - 0.136 log r), where Δ_c and Δ_o are the corrected and observed densities respectively and r is the distance of the detector from core. Corrected observed densities as a function of core distance for different shower sizes are shown in figures 'lateral distribution of electrons'. Representative sets of our results with the comparison of NKG[10] structure function

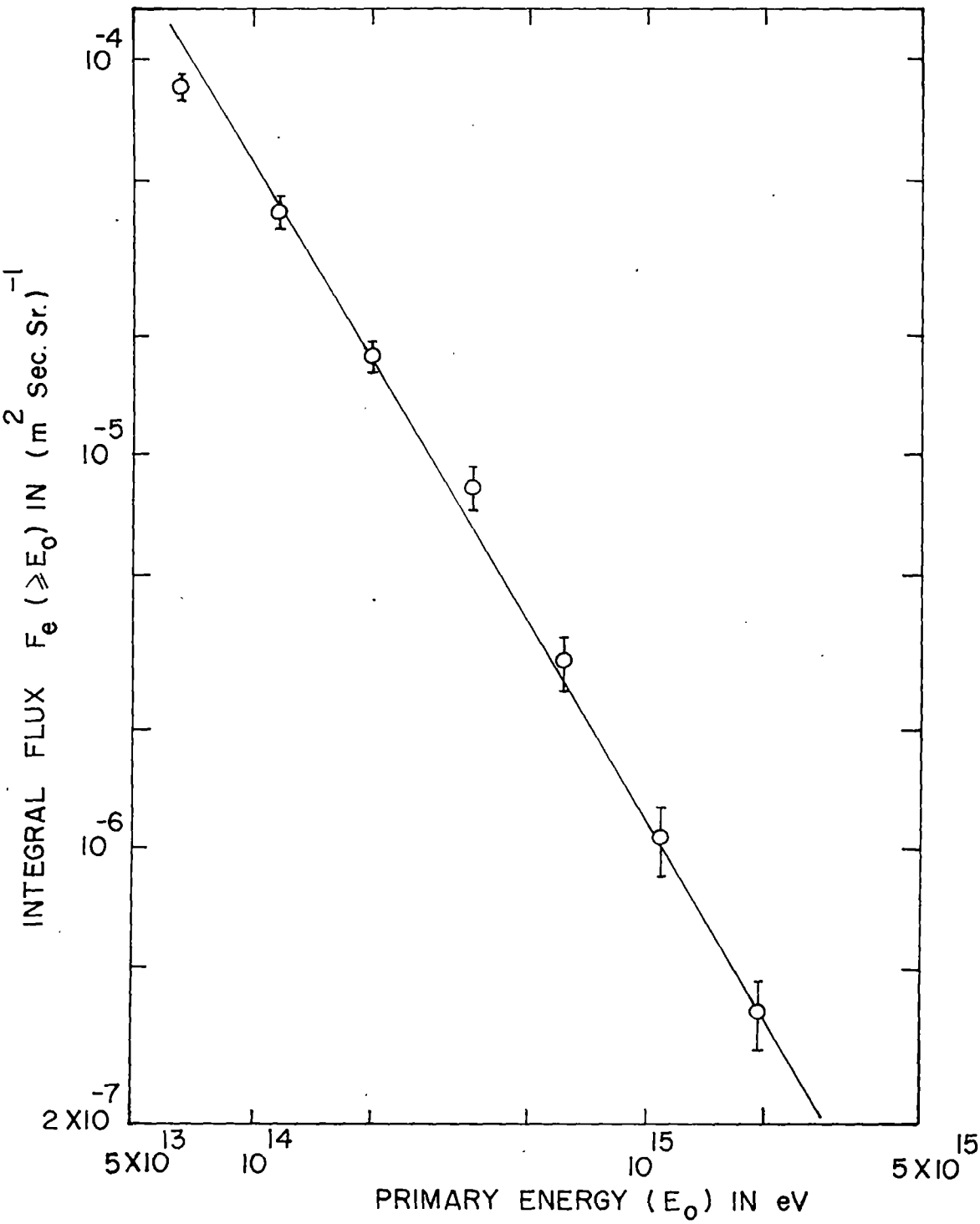

Fig. 5.3 OBSERVED INTEGRAL ENERGY SPECTRUM OF PRIMARY COSMIC RAYS FROM ELECTRON-SIZES

and Hillas[3] structure function for four small shower size groups are shown in figure 5.4-5.7. The error bars are purely statistical. The observed distributions are in good agreement with that of expected lateral distribution of Hillas et al[3] out to a distance 25 m.

5.5 Muon density in showers

The muons are detected by magnetic spectrograph placed within the array. The effective threshold for muons associated with an EAS in the near vertical direction is 2.5 GeV. Selected showers are divided in groups according to their sizes and the distance r between the shower axis and the registered muons in the same horizontal plane. All the showers with age between 0.8 to 1.3 are considered for this selection. All the recorded muons are then subdivided according to different threshold energy.

5.5.1 Estimation of muon density

In the present experiment the muon density $(\bar{\rho}_\mu(\geq E_\mu, r)$ is obtained by purely statistical way. Let $N(N_e, r)$ be the total number of recorded showers with average size N_e having mean core distance from the muon detector r and $n_\mu(N_e, r)$ be the number of muons detected by the magnetic spectrographs with effective area A_μ within those showers, then the average density of muons for that average value of N_e and r is given by

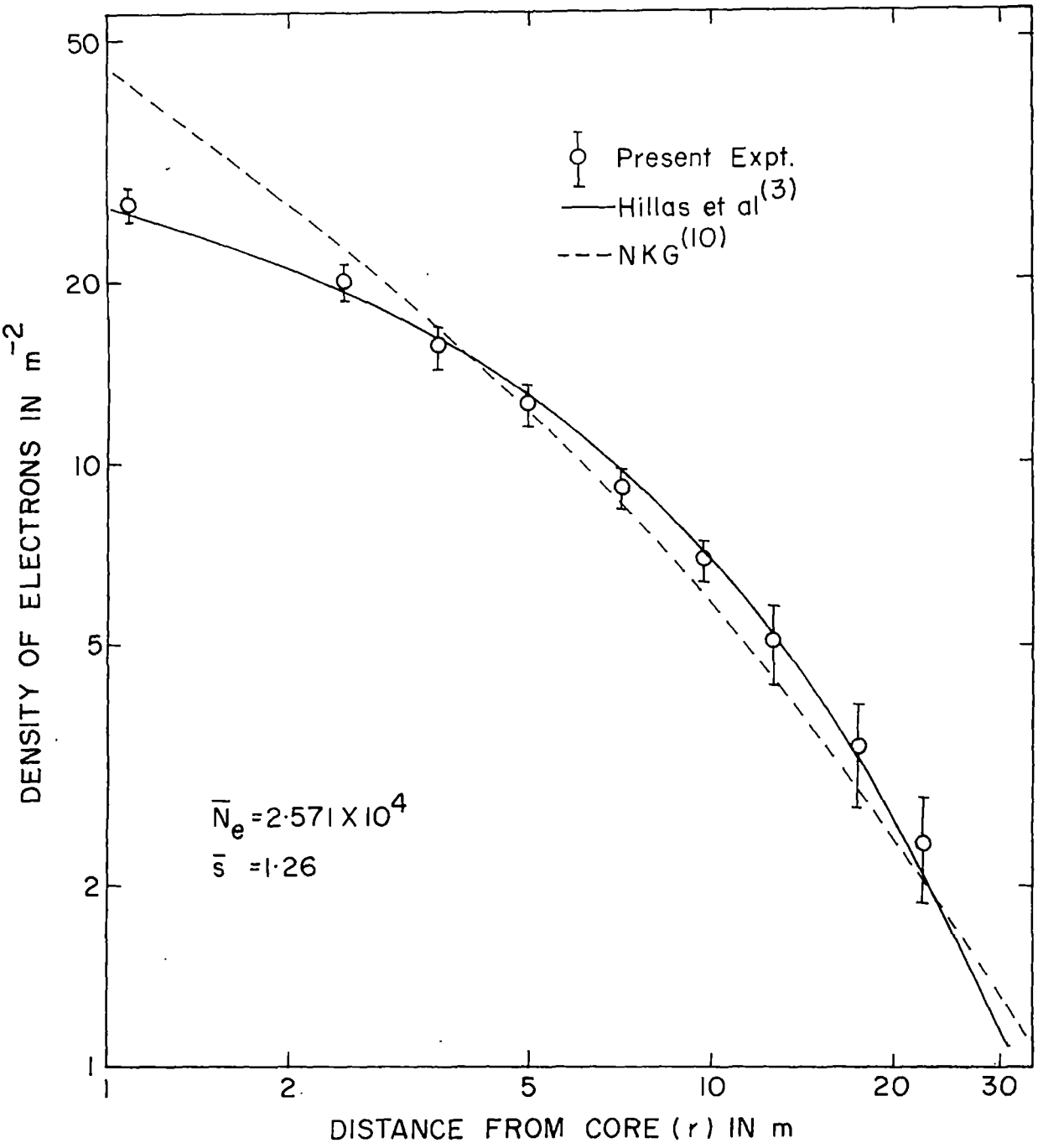

Fig. 5·4 LATERAL DISTRIBUTION OF ELECTRONS IN THE SHOWER SIZE RANGE $(2-3) \times 10^4$

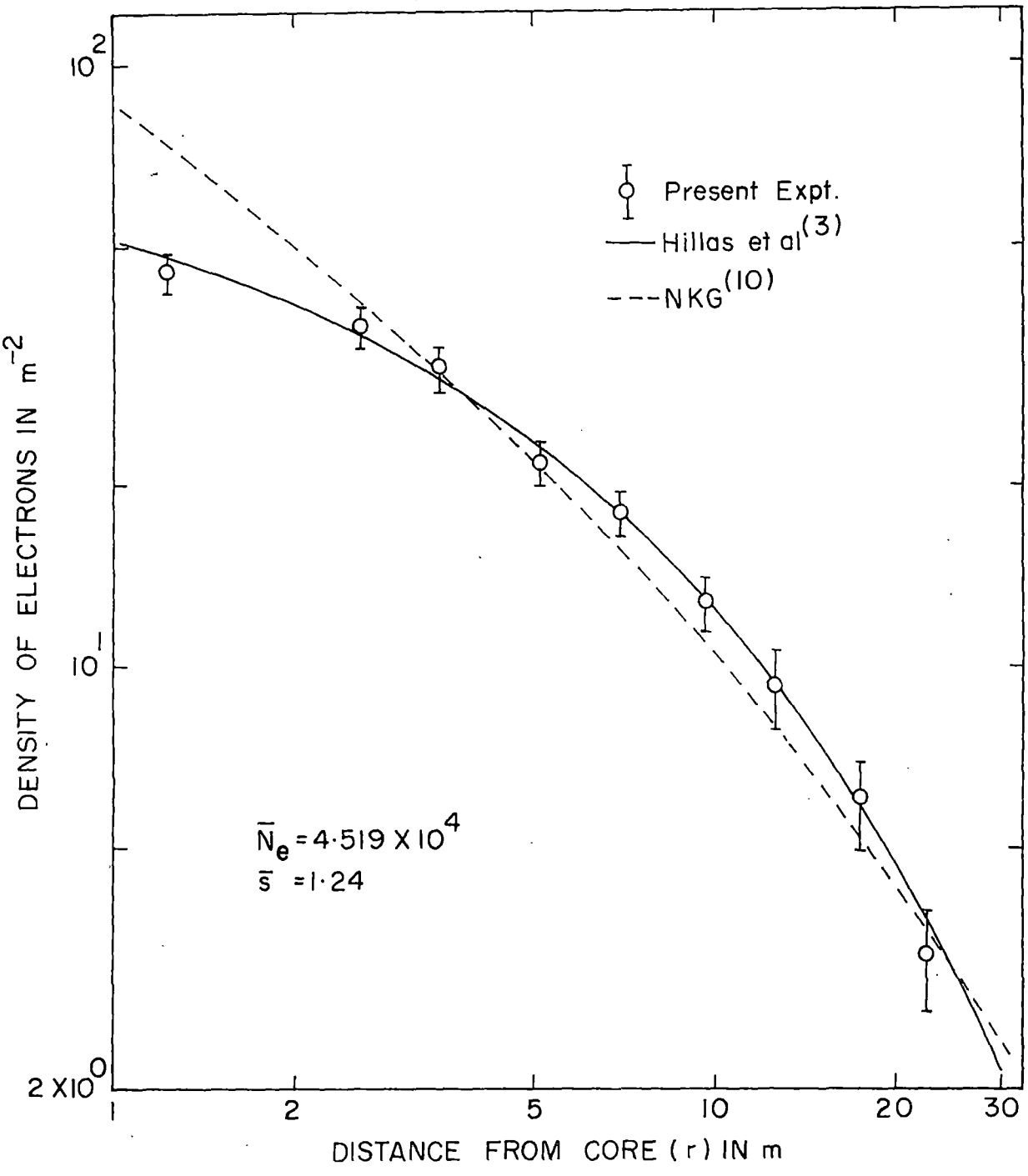

Fig. 5·5 LATERAL DISTRIBUTION OF ELECTRONS IN THE SHOWER SIZE RANGE $(4-5) \times 10^4$

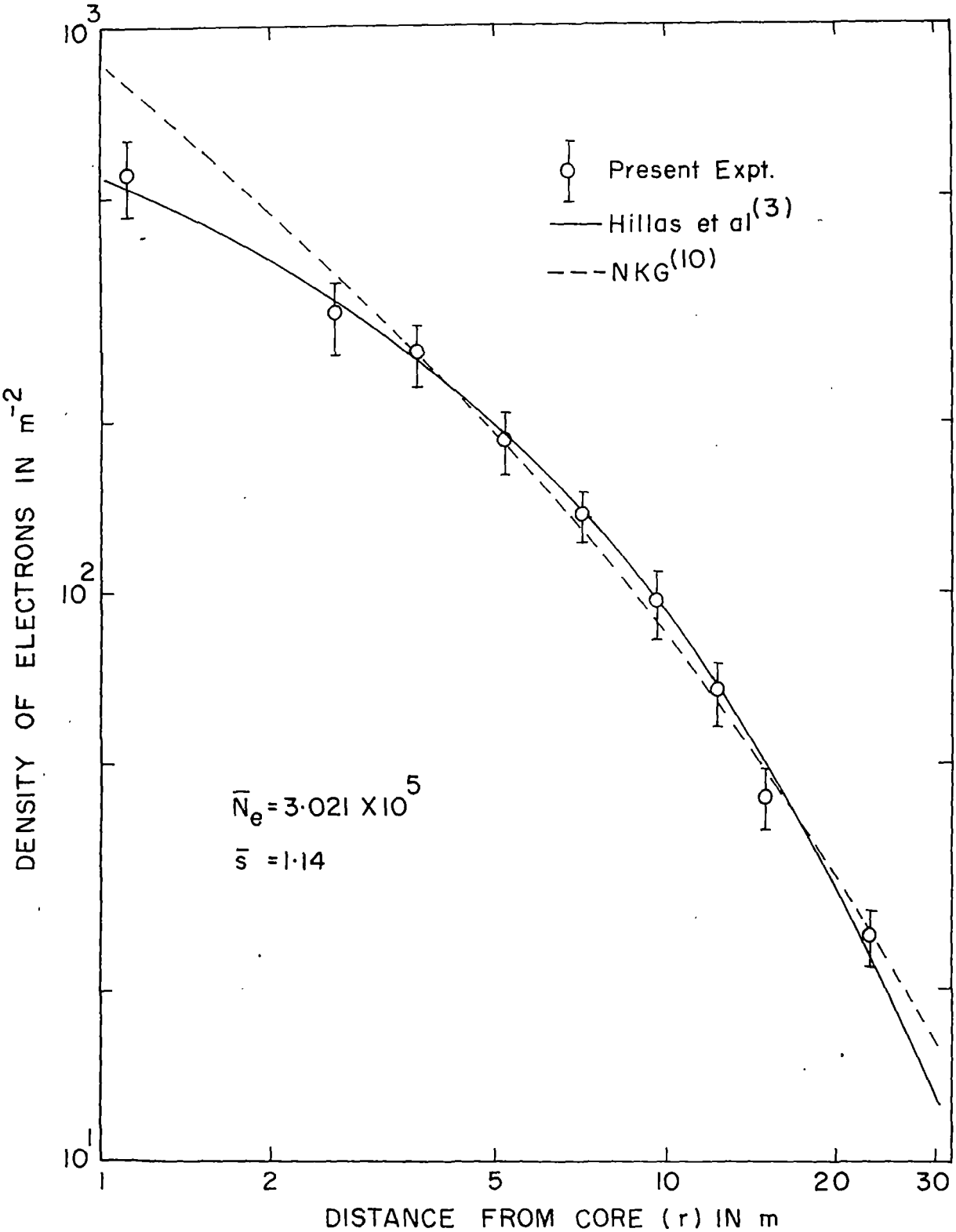

Fig. 5·6 LATERAL DISTRIBUTION OF ELECTRONS IN THE SHOWER SIZE RANGE $(2-4) \times 10^5$

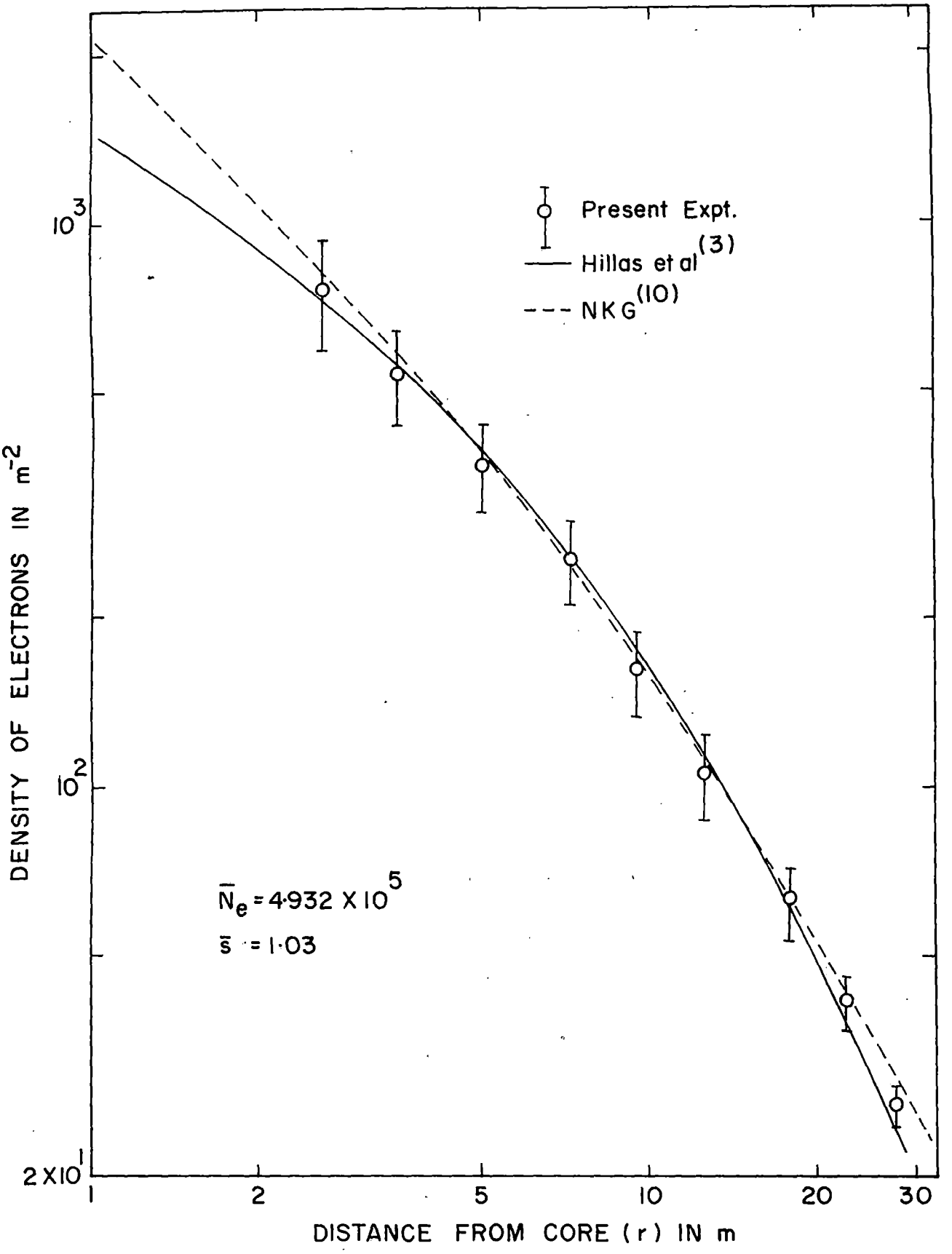

Fig. 5·7 LATERAL DISTRIBUTION OF ELECTRONS IN THE SHOWER SIZE RANGE $(4-6) \times 10^5$

$$\rho_\mu(N_e,r) = \frac{n_\mu(N_e,r)}{N(N_e,r)A_\mu} \quad \ldots \quad \ldots \quad (5.9)$$

The effective area of the muon detector A_μ is approximately equal for all the muons observed since the maximum projected angle by the magnetic spectrograph is very low (i.e., near vertical).

5.5.2 Lateral distribution of muons in showers

Showers are divided into seven groups according to their sizes and each size bin are subdivided into 12 distance bins with lowest distance bin of 4 m. The density of muons for threshold energies 2.5 GeV, 11.3 GeV, 25.5 GeV and 53.7 GeV are then calculated by using the equation (5.9). The lateral distribution of muons for seven shower size groups and for four threshhold energies are shown in figure 5.8 - 5.14. The error bars given on the density of muons are based on the number of muons in each distance bin and the parameters involved in the density measurements. In figure 5.15 the lateral distribution of muons for seven different shower sizes with the energy threshold 25.5 GeV is given. The experimental data are approximated by the equation of the form $\rho_\mu(r) = Ar^{-\alpha}\exp(-\frac{r}{r_o})$ in the narrow interval $\frac{\Delta N_e}{N_e} \approx 0.67$ of shower size. The fitted function is represented by the smooth lines in figure 5.8 - 5.14. Figure 5.15 shows that the slope of lateral distribution increases with shower size. In table 5.1 the best fit value of the constants A, α and r_o for different shower sizes and threshold energies are given :

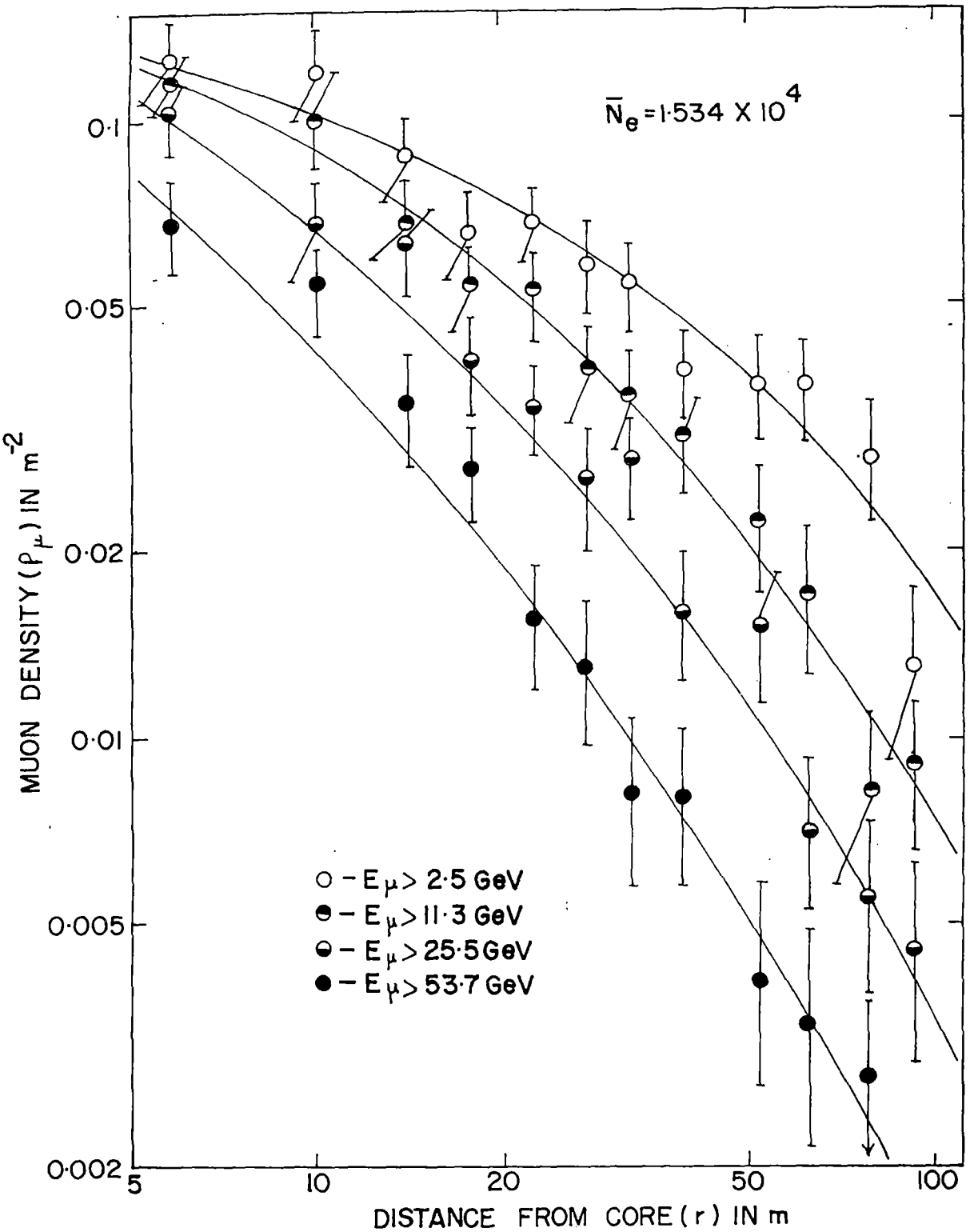

Fig. 5.8 LATERAL DISTRIBUTION OF MUONS IN EAS FOR DIFFERENT MUON ENERGY THRESHOLD IN THE SHOWER SIZE RANGE $(1-2) \times 10^4$ PARTICLES. THE LEAST-SQUARES FIT TO THE DATA ARE SHOWN AS SOLID LINES

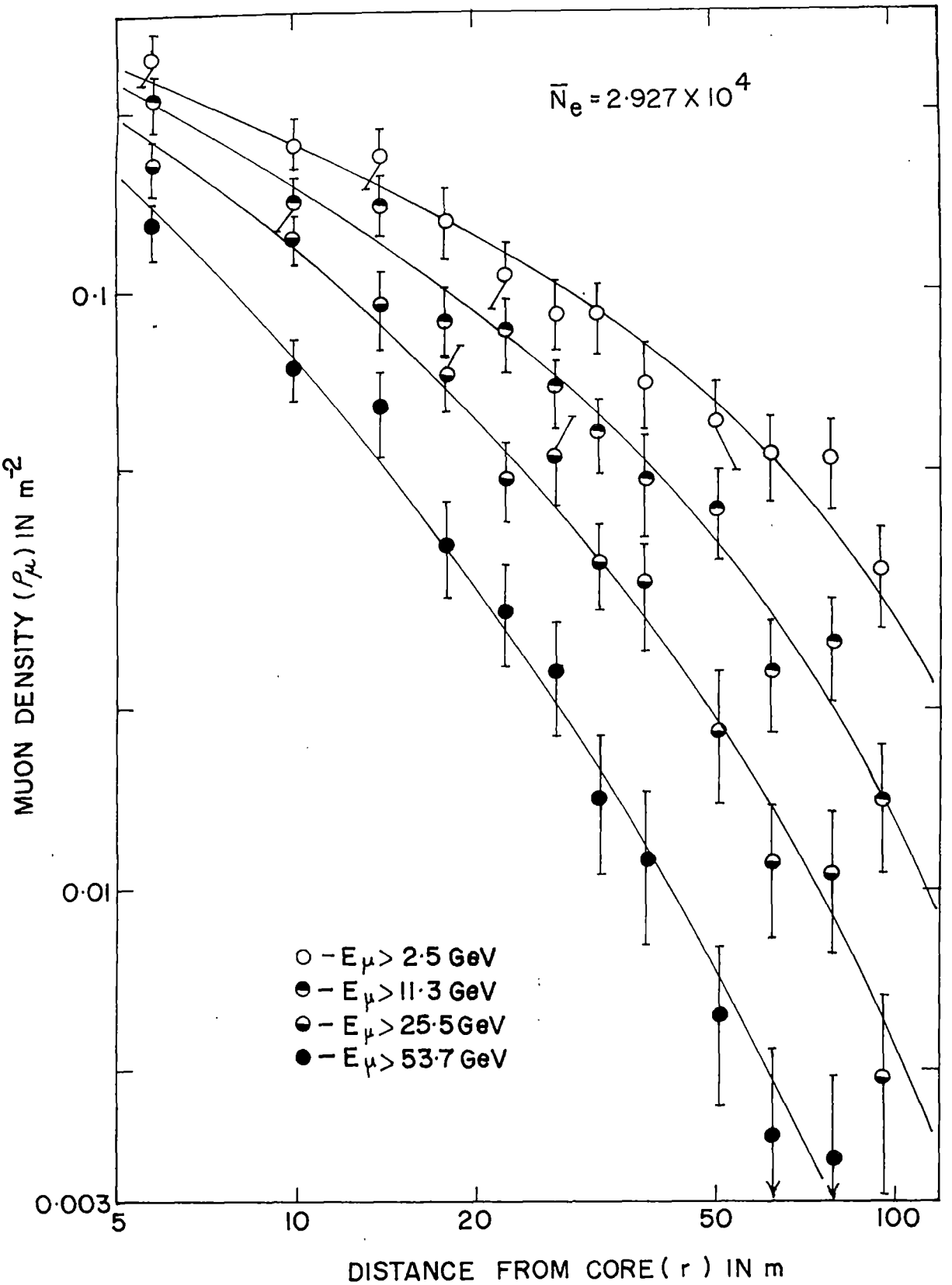

Fig. 5.9 LATERAL DISTRIBUTION OF MUONS IN EAS FOR DIFFERENT MUON ENERGY THRESHOLD IN THE SHOWER SIZE RANGE (2-4) x 10^4 PARTICLES. THE LEAST-SQUARES FIT TO THE DATA ARE SHOWN AS SOLID LINES.

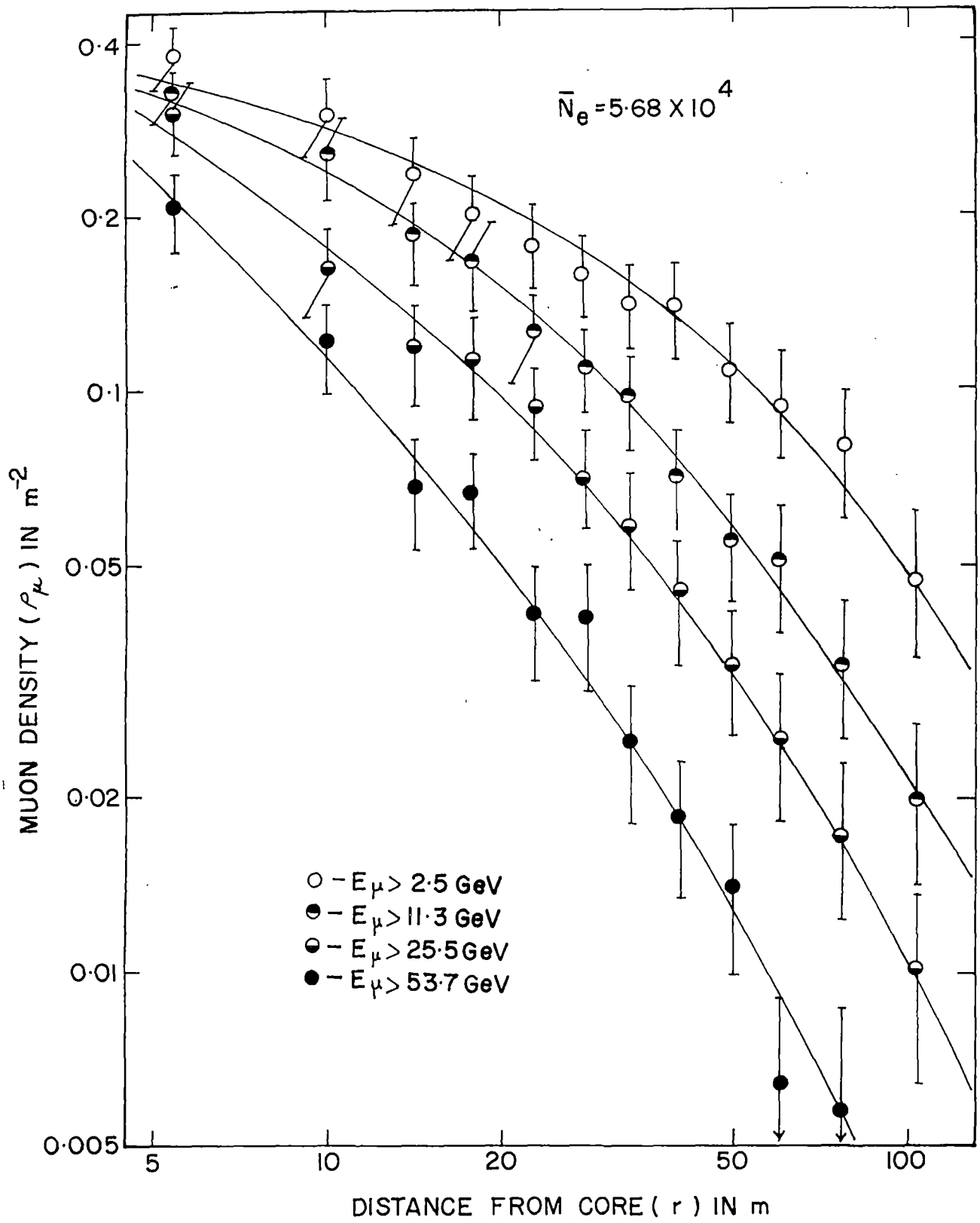

Fig.5.10. LATERAL DISTRIBUTION OF MUONS IN EAS FOR DIFFERENT MUON ENERGY THRESHOLD IN THE SHOWER SIZE RANGE (4-8) x 10^4 PARTICLES. THE LEAST-SQUARES FIT TO THE DATA ARE SHOWN AS SOLID LINES.

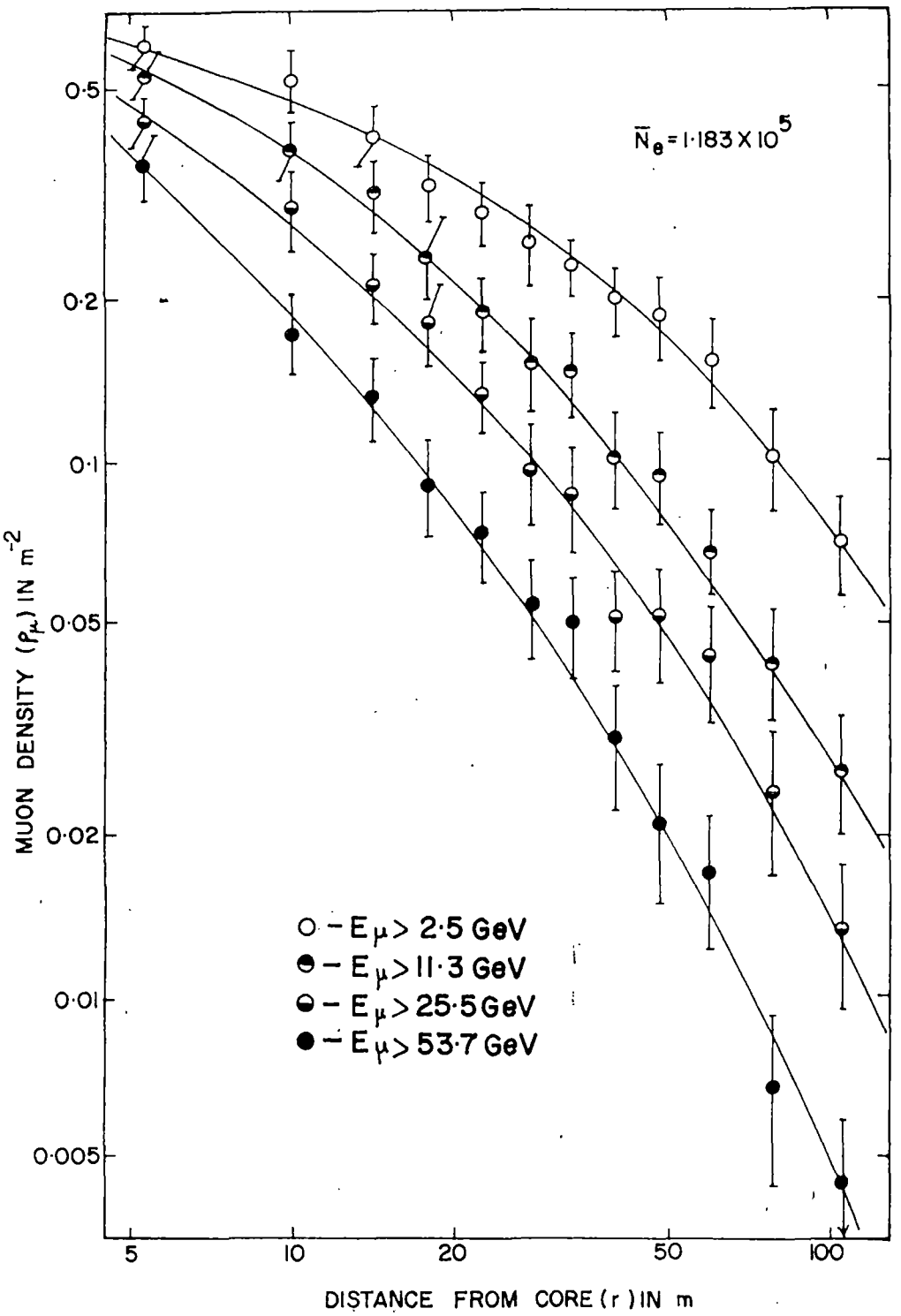

Fig.5.11. LATERAL DISTRIBUTION OF MUONS IN EAS FOR DIFFERENT MUON ENERGY THRESHOLD IN THE SHOWER SIZE RANGE (8-16) x 10^4 PARTICLES. THE LEAST-SQUARES FIT TO THE DATA ARE SHOWN AS SOLID LINES.

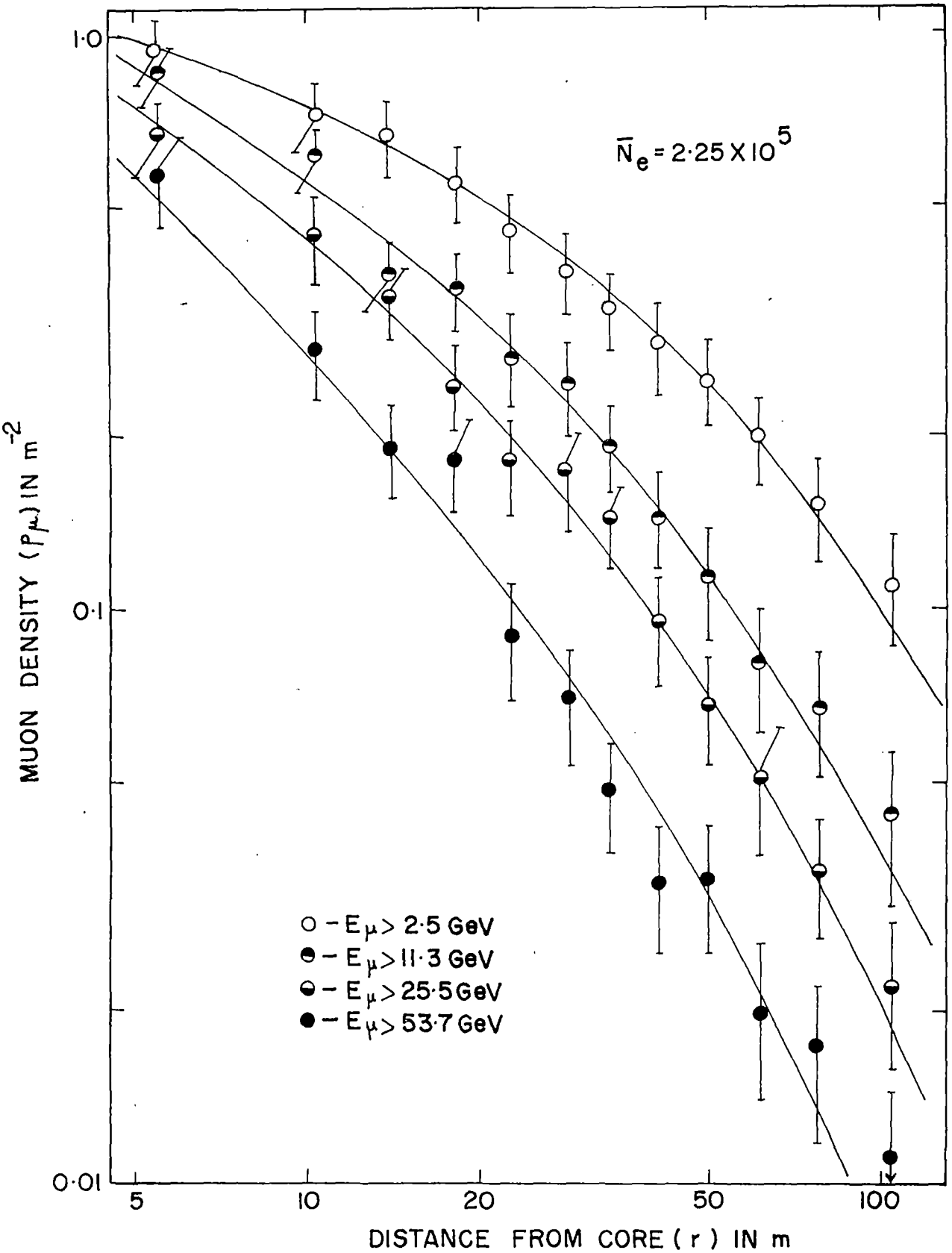

Fig.5.12. LATERAL DISTRIBUTION OF MUONS IN EAS FOR DIFFERENT MUON ENERGY THRESHOLD IN THE SHOWER SIZE RANGE (1.6-3.2) x 10^5 PARTICLES. THE LEAST-SQUARES FIT TO THE DATA ARE SHOWN AS SOLID LINES.

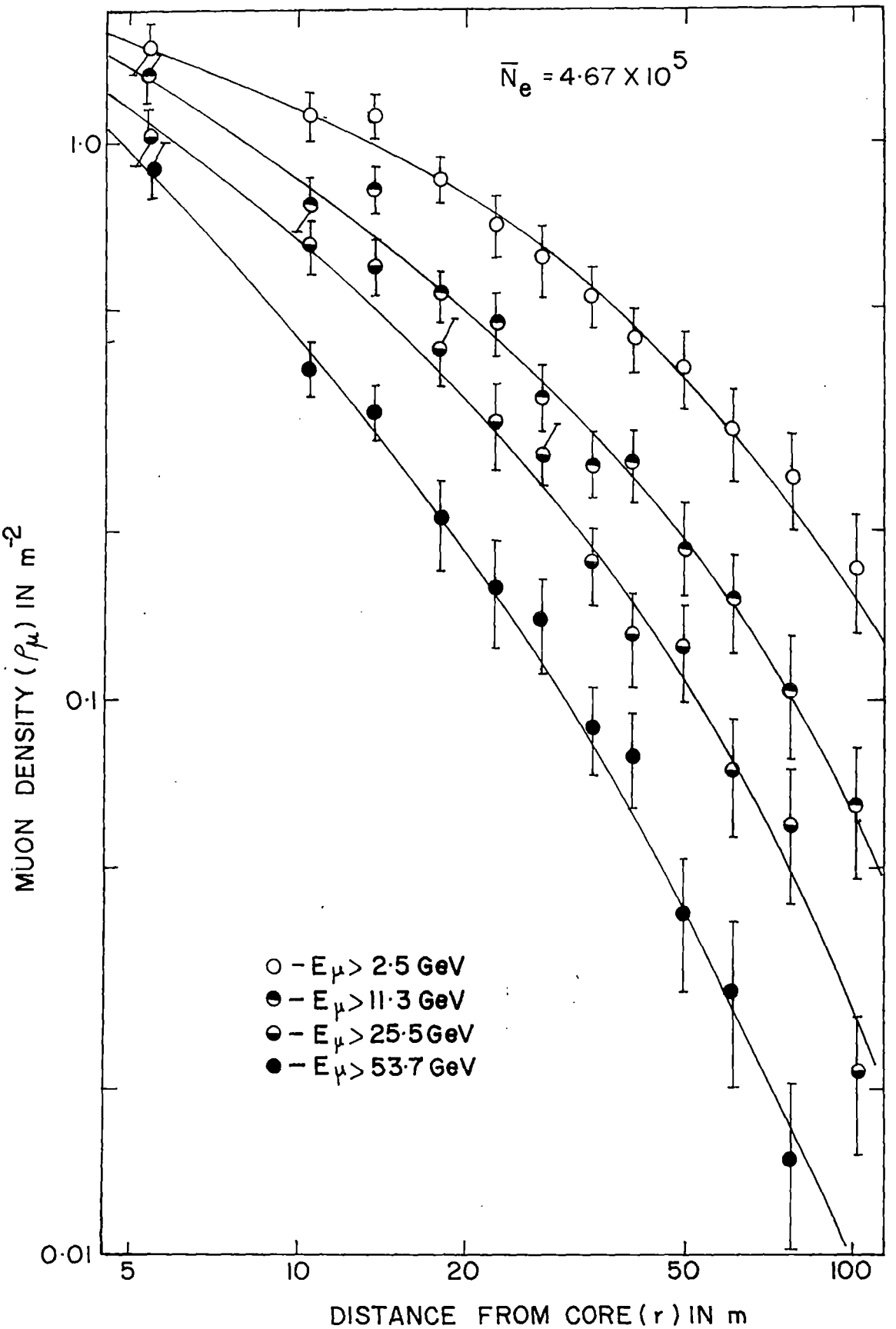

Fig.5.13. LATERAL DISTRIBUTION OF MUONS IN EAS FOR DIFFERENT MUON ENERGY THRESHOLD IN THE SHOWER SIZE RANGE (3.2-6.4) x 10^5 PARTICLES. THE LEAST-SQUARES FIT TO THE DATA ARE SHOWN AS SOLID LINES.

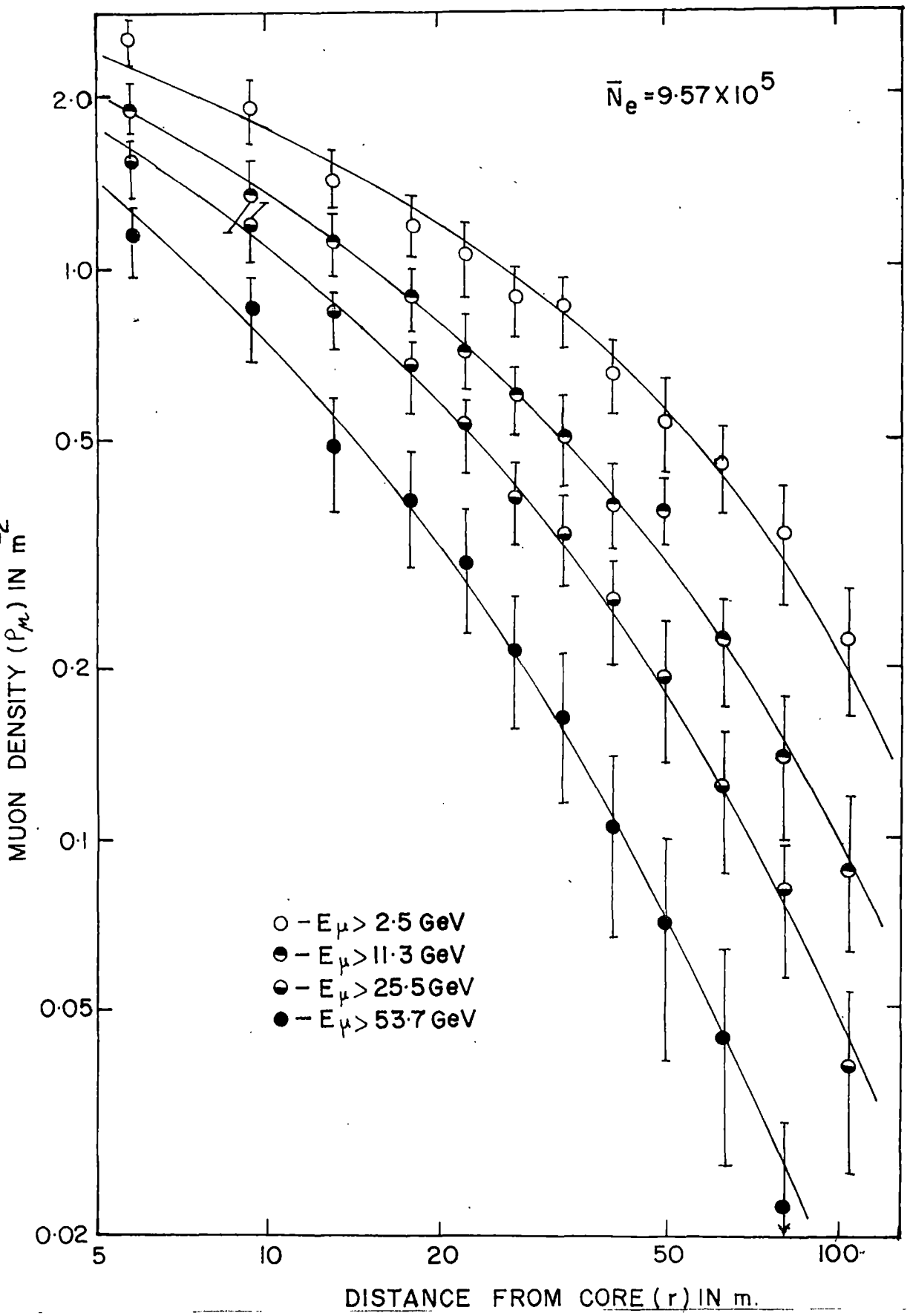

Fig.5.14. LATERAL DISTRIBUTION OF MUONS IN EAS FOR DIFFERENT MUON ENERGY THRESHOLD IN THE SHOWER SIZE RANGE (6.4-12) x 10^5 PARTICLES. THE LEAST-SQUARES FIT TO THE DATA ARE SHOWN AS SOLID LINES.

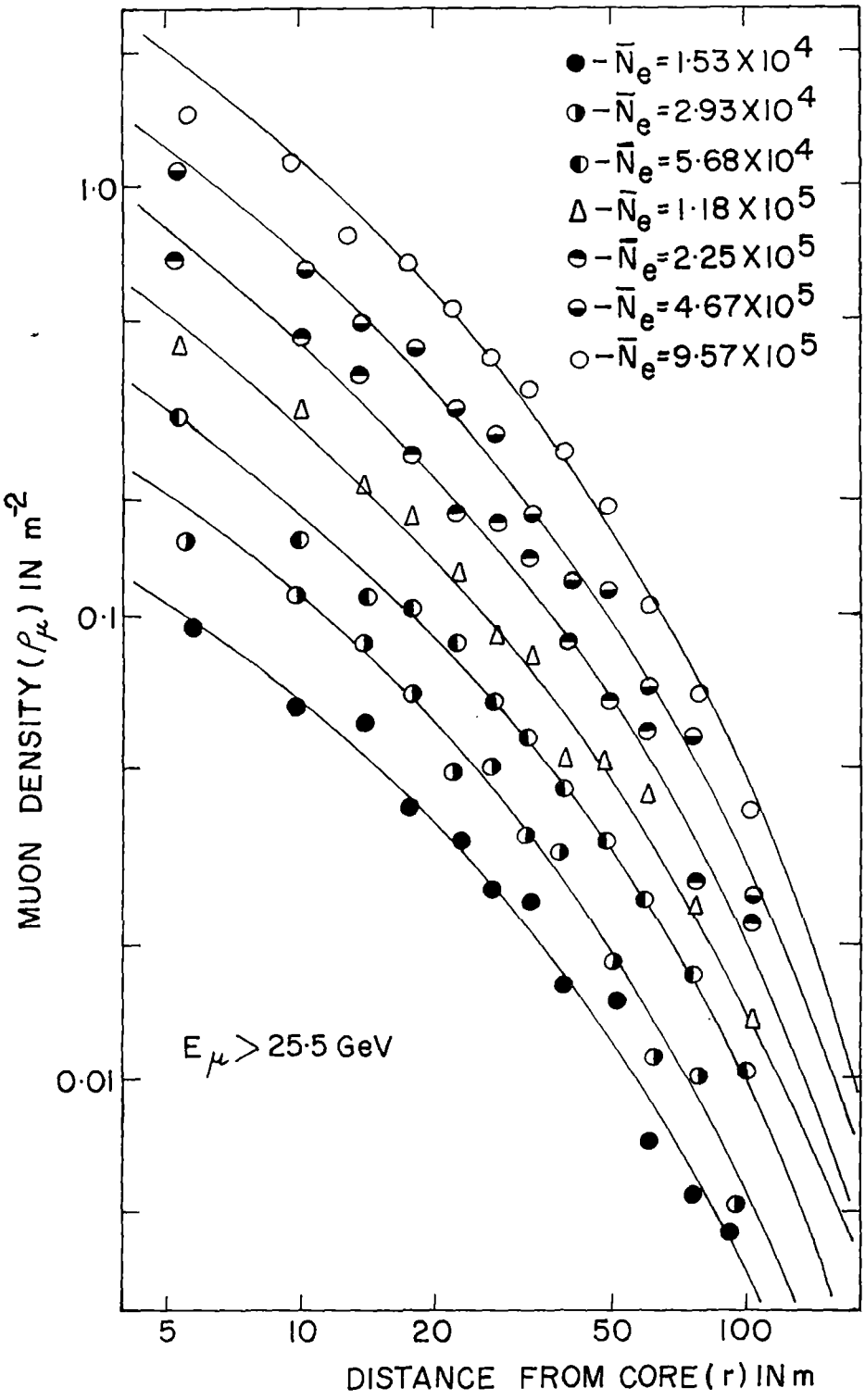

Fig. 5.15 LATERAL DISTRIBUTION OF MUONS IN EAS FOR DIFFERENT SHOWER SIZES WITH THE MUON ENERGY THRESHOLD 25.5 GeV. SOLID LINES ARE THE BEST FIT TO THE DATA.

TABLE 5.1

Shower size ($\bar{N}_e$)	Muon energy threshold ($>E_\mu$) in GeV	r_o	A	α
1.534×10^4	2.5	80.92	0.209 ± 0.023	0.260 ± 0.028
	11.3		0.422 ± 0.043	0.608 ± 0.029
	25.5		0.482 ± 0.065	0.798 ± 0.041
	53.7		0.434 ± 0.066	0.970 ± 0.049
2.927×10^4	2.5	78.68	0.378 ± 0.037	0.280 ± 0.029
	11.3		0.579 ± 0.057	0.533 ± 0.029
	25.5		0.935 ± 0.112	0.834 ± 0.036
	53.7		1.283 ± 0.192	1.150 ± 0.051
5.680×10^4	2.5	76.37	0.570 ± 0.041	0.255 ± 0.025
	11.3		0.952 ± 0.070	0.540 ± 0.022
	25.5		1.040 ± 0.042	0.710 ± 0.016
	53.7		1.320 ± 0.106	1.011 ± 0.031
1.183×10^5	2.5	73.82	1.030 ± 0.058	0.280 ± 0.018
	11.3		1.660 ± 0.100	0.585 ± 0.017
	25.5		1.825 ± 0.151	0.751 ± 0.026
	53.7		2.540 ± 0.259	1.060 ± 0.033

.....table contd.

contd. from previous page

2.250×10^5	2.5	71.60	1.654 ± 0.066	0.302 ± 0.013
	11.3		2.487 ± 0.184	0.594 ± 0.015
	25.5		3.133 ± 0.285	0.789 ± 0.027
	53.7		2.744 ± 0.420	0.951 ± 0.044
4.670×10^5	2.5	69.05	2.620 ± 0.185	0.293 ± 0.022
	11.3		3.663 ± 0.171	0.563 ± 0.024
	25.5		4.869 ± 0.452	0.788 ± 0.026
	53.7		6.260 ± 0.473	1.075 ± 0.021
9.573×10^5	2.5	66.6	4.440 ± 0.382	0.333 ± 0.028
	11.3		5.631 ± 0.289	0.550 ± 0.015
	25.5		7.251 ± 0.293	0.748 ± 0.013
	53.7		9.370 ± 0.681	1.050 ± 0.023

5.6 Size dependence of total number of muons

All the showers are divided into 7 groups with the size bin $(1\text{-}2) \times 10^4$, $(2\text{-}4) \times 10^4$, $(4\text{-}8) \times 10^4$, $(8\text{-}16) \times 10^4$, $(1.6\text{-}3.2) \times 10^5$, $(3.2\text{-}6.4) \times 10^5$, $(6.4\text{-}12) \times 10^5$. Each shower group is again subdivided into 12 radial groups out to 120 m such that the smallest bin is of width 4 m. The total number of muons for each shower size group is then calculated by the relation

$$N_\mu = \sum_i \rho_\mu^i(r)\, A_i \quad \ldots \quad \ldots \quad (5.10)$$

where $\rho_\mu^i(r)$ is the density of muons in the ith distance bin having the annular area A_i. The N_μ value is calculated for five different threshold energy of muons. The variation of muon size with the shower size for the energy threshold 2.5 GeV, 11.3 GeV, 25.5 GeV and 53.7 GeV are shown in figure 5.16. The errors on N_μ in figure are purely statistical. All the data for each energy threshold are fitted with the equation of the form $N_\mu = A \left(\frac{N_e}{10^4} \right)^\alpha$. The coefficients A and α for different energy threshold is given in table 5.2.

TABLE 5.2

Muon energy threshold ($>E_\mu$) in GeV	A	α
2.5	$(8.686 \pm 0.228) \times 10^2$	0.630 ± 0.021
11.3	$(5.493 \pm 0.121) \times 10^2$	0.634 ± 0.014
25.5	$(2.990 \pm 0.051) \times 10^2$	0.659 ± 0.012
53.7	$(0.993 \pm 0.050) \times 10^2$	0.670 ± 0.060

The smooth lines for different primary mass number and the dashed line for proton primary from the results of MSU group[11] are compared with our results (open circle) in figure 5.17 for the energy threshold 10 GeV. In table 5.3 a comparison of our results with those obtained from Monte Carlo simulation data for proton primary is given.

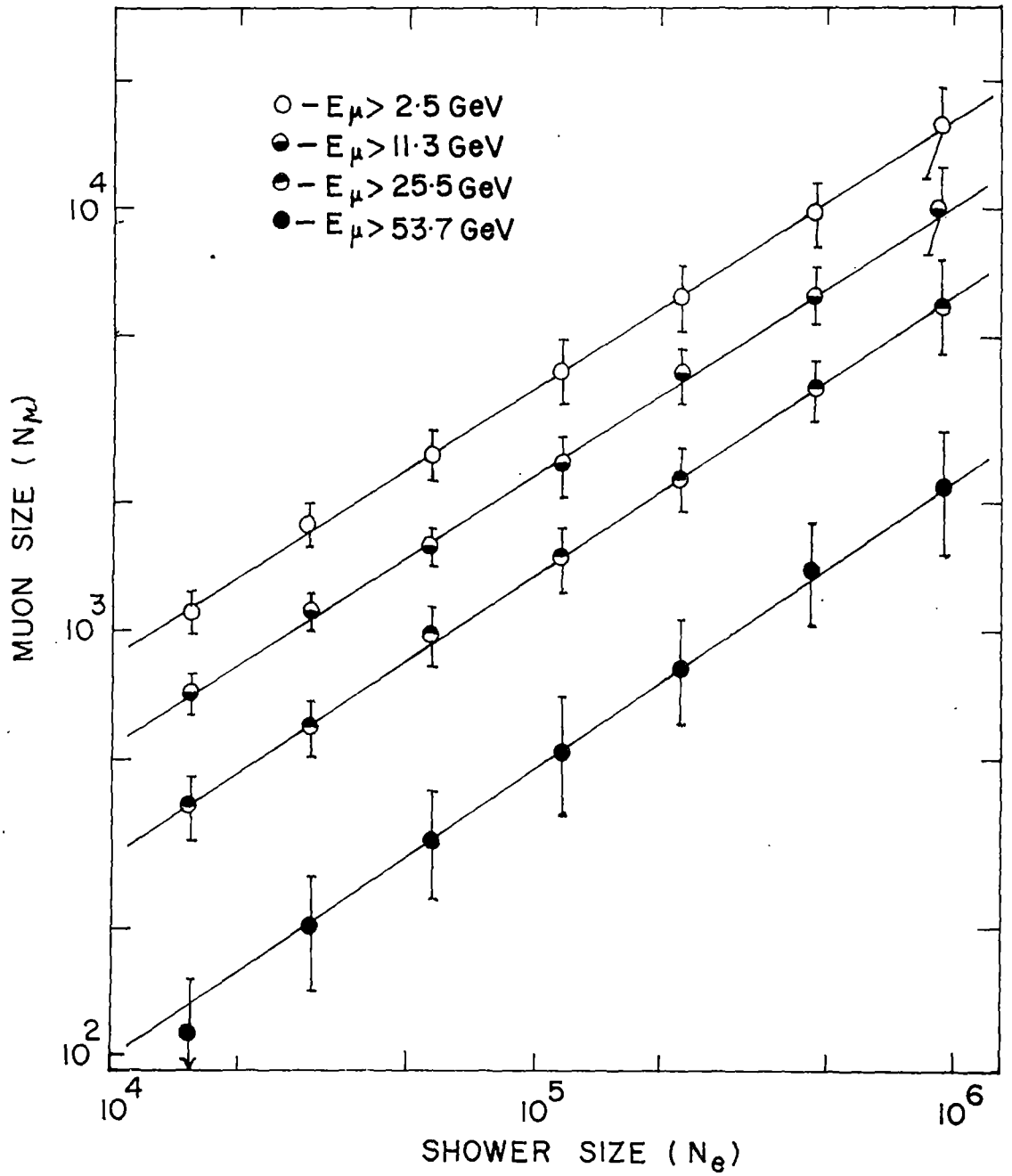

Fig. 5.16 VARIATION OF MUON SIZES (N_μ) WITH SHOWER SIZES (N_e) FOR DIFFERENT MUON ENERGY THRESHOLD. THE SOLID LINES ARE THE BEST FIT TO THE DATA.

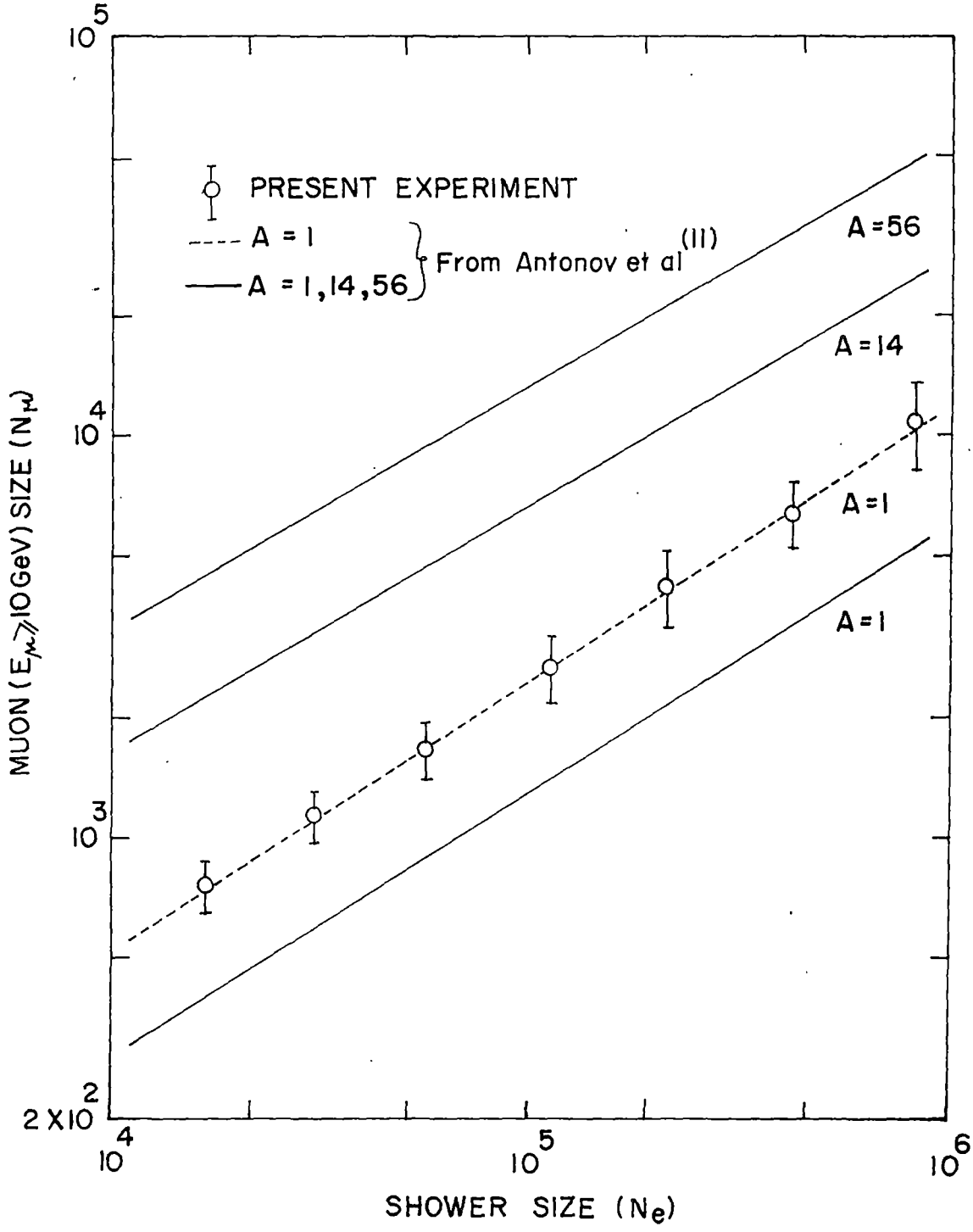

Fig. 5.17 COMPARISON OF PRESENT RESULTS OF SIZE DEPENDENCE OF MUON ($E_\mu > 10$ GeV) TO ELECTRON WITH THE RESULTS OF ANTONOV *et al* (11) FOR DIFFERENT PRIMARY MASS NUMBERS.

TABLE 5.3

Present Experiment of NBU Array E_μ>2.5 GeV			Monte Carlo simulation[12], E_μ>2 GeV (proton primary)		
E_o in eV	N_e	N_μ	E_o in eV	N_e	N_μ
9.38×10^{13}	1.53×10^{4}	1.11×10^{3}	1×10^{14}	1.08×10^{4}	1.55×10^{3}
4.91×10^{14}	1.18×10^{5}	4.25×10^{3}	5×10^{14}	8.80×10^{4}	6.60×10^{3}
1.50×10^{15}	4.67×10^{5}	9.81×10^{3}	2×10^{15}	5.39×10^{5}	2.24×10^{4}
2.67×10^{15}	9.57×10^{5}	1.60×10^{4}			

The comparison of our results on muon number (E_μ>2.5 GeV) with those for muons (E_μ>2 GeV) from Monte Carlo calculations of Wrotniak and Yodh[12] and with the calculations of Antonov et al[11] on additive quark model has set a level of confidence in the process of extracting the primary composition from air shower observations.

5.7 Discussion

Hillas[3] structure function is used to obtain the shower parameters (N_e, s, X_o, Y_o) for each shower by density values of 21 points. The average value of age ($\bar{s}$) for each group of showers is ploted as a function of shower size in figure 5.1 along with the results of Akeno group[1] and KGF experiment[2]. The age parameter ($\bar{s}$) in the present experiment is consistent with other measurements[1,2].

Lateral distribution of electrons at different shower size ranges are shown in figures 5.4-5.7. The observed values of electron densities at different distances from the core are in better agreement with Hillas[3] structure function than with NKG[10] function out to a distance 25 m.

The lateral distribution of muons for different muon energy threshold, presented in figure 5.8-5.14 is fitted with the equation of the form

$$\rho_\mu(r) = Ar^{-\alpha}\exp(-r/r_o)$$

The value of α for all the size range and the energy threshold upto 53.7 GeV is within 0.26 to 1.06. The parameter α seen to be nearly independent of shower size [value of α is presented in table 5.1] which is also concluded by different workers[13-15].

A comparison of shower size dependence of total number of muons for the muon energy threshold 10 GeV is presented in figure 5.17. The slope of the observed result is in excellent agreement with the results presented by Antonov et al[11]. By this figure and compairing the Monte Carlo simulated data [Wrotniak et al[12]] with the observed values [presented in table 5.3], it can be concluded that the proton primary is dominant in the primary energy range $5 \times 10^{13} - 2 \times 10^{15}$ eV.

A comparison of present primary energy spectrum from electron sizes with the direct measurement of Grigorov et al[16]

is given in figure 5.18. The measured absolute values as well as the slope of the curves are in agreement with the direct measurements obtained with proton satellite by Grigorov[16] at the present primary energy range.

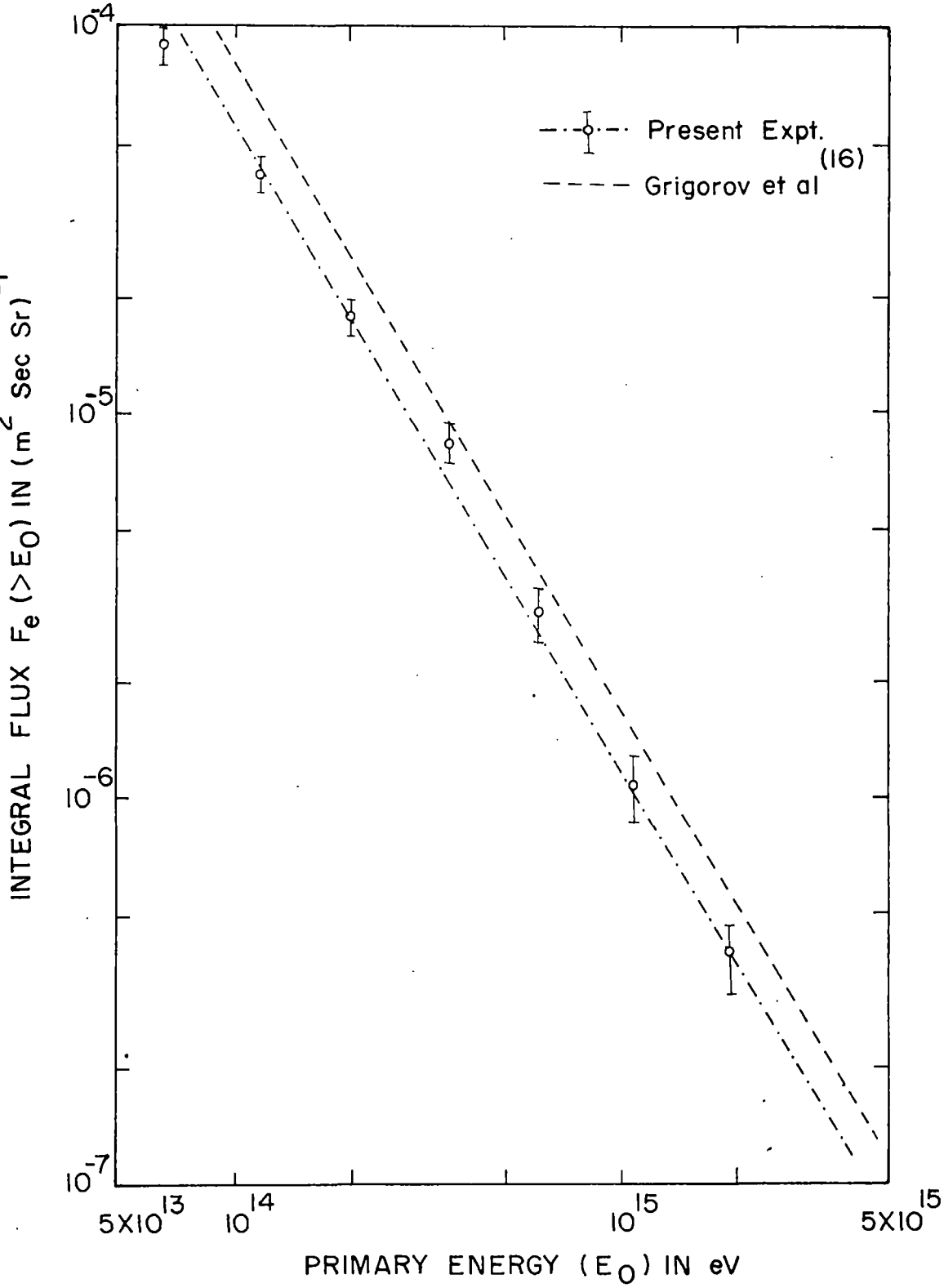

Fig.5·18 INTEGRAL ENERGY SPECTRUM OF COSMIC RADIATION FROM ELECTRON-SIZES.

References

1. Hara, T., Hatano, Y., Hayashida, N., Jogo, N., Kamata, K., Kifune, T., Mizumoto, Y., Nagno, M., Tanahashi, G., Tan, Y.H., Kawaguchi, S., Daigo, M. and Hasebe, N., Proc. 17th ICRC, Paris, 11(1981)52.
2. Acharya, B.S., Ph.D Thesis, Bombay, India, 1983.
3. Hillas, A.M. and Lapikens, J., Proc. 15th ICRC, Plovdiv, 8(1977)460.
4. Kameda, T., Maida, T. and Toyoda, Y., Proc. 6th ICRC, Moscow, 2(1959)58.
5. McCusker, C.B.A., Proc. 7th ICRC, Tokyo, 3(1961)293.
6. Dedenko, L.G., 14th ICRC, Munich, 8(1975)2857
7. Hara, T., Hayashida, N., Honda, M., Ishikowa, F., Kamata, K., Kifune, T., Mizumoto, Y., Nagano, M., Tanahashi, G. and Teshima, M., Proc. 18th ICRC, Bangalore, 9(1983)198
8. Srikantha Rao, Ph.D. Thesis, Bombay, India, 1981
9. Asakimori, K., Hata, T., Maeda, T., Nishijima, K., Toyoda, Y., Kamamoto, K., Yoshida, M., Kameda, T and Mizushima, K., Proc. 17th ICRC, Paris, 11(1981)301
10. Greisen, K., Ann.Rev.Nuc.Sci., 10(1960)63
11. Antonov, R.A., Ivanenko, I.P., Kanevsky, B.L., Kuzmin, V.A. and Roganova, T.M., Proc. 18th ICRC, Bangalore, 6(1983)159
12. Wrotniak, J.A. and Yodh, G.B., Proc. 19th ICRC, La-Jolla, 7(1985)1

13. Aseikin, V.S., Dulovij, A.G., Kabanova, N.V., Nesterova, N.M., Nikolskaya, N.M., Nikolsky, S.I., Romachin, V.A., Tukish, E.I., Katsarsky, L.M., Kirov, I.N., Stamenov, J.N. and Janminchev, V.D., Proc. 15th ICRC, Plovdiv, 8(1977)98

14. Machavariani, S.K., Nikolsky, S.I. and Tukish, E.I., Proc. 16th ICRC, Kyoto, 8(1979)240

15. Abdrashitov, S.F., Bjurina, T.A., Vavilov, Y.N., Duboviy, A.G., Djatlov, P.A., Marinenko, V.A., Nesterova, N.M., Nikolskaja, N.M., Serdjukov, A.D., Tukish, E.I., Yakovlev, V.I., Kirov, T.N., Sariev, D.B., Stamenov, I.N. and Ushev, S.Z., Proc. 17th ICRC, Paris, 6(1981)156

16. Grigorov, N.L., Gubin, Yu.V., Rapoport, I.D., Savenko, I.A., Yakovlev, B.M., Akimov, V.V. and Nesterov, V.E., Proc. 12th ICRC, Hobart, 5(1971)1746.